mathematics

Article

A Heuristic Approach for Multi-Path Signal Progression Considering Traffic Flow Uncertainty

Tianrui Hai †, Gang Ren *, Weihan Chen †, Qi Cao and Changyin Dong

School of Transportation, Southeast University, Jiulonghu Campus, Nanjing 211100, China
* Correspondence: rengang@seu.edu.cn; Tel.: +86-25-13851664823; Fax: +86-25-52091277
† These authors contributed equally to this work.

Abstract: The multi-path progression of an arterial signal model, generally, is applied to arterial traffic scenarios with large turning flows. However, existing methods generally fail to capture traffic flow uncertainty, which leads to high sensitivity to fluctuations in traffic flow. To bridge this gap, in this study, a heuristic approach for multi-path signal progression is proposed to deal with the uncertainties of flow fluctuation by using distributionally flow scenarios. The model varies the phase sequence and the offsets of each intersection to achieve optimal progression with weighting of efficiency and stability. The preference degree of the efficiency and stability of the model is selected by adjusting the efficiency stability coefficient and solved by using a genetic algorithm. A case study and comparison experiment with benchmark models is presented and analyzed to prove the advantages of the proposed model. The results show that the standard deviation of the proposed model decreases by 45% as compared with conventional methods. It indicates that the model proposed in this paper can reduce congestion due to uncertainties, and can significantly improve stability, on the premise of ensuring that the efficiency index maintains a better value.

Keywords: multi-path progression; heuristic approach; traffic flow uncertainty; green band

MSC: 90C17

check for updates

Citation: Hai, T.; Ren, G.; Chen, W.; Cao, Q.; Dong, C. A Heuristic Approach for Multi-Path Signal Progression Considering Traffic Flow Uncertainty. *Mathematics* **2023**, *11*, 377. https://doi.org/10.3390/math11020377

Academic Editor: Andrea Scozzari

Received: 21 November 2022
Revised: 6 January 2023
Accepted: 7 January 2023
Published: 10 January 2023

1. Introduction

Currently, research on signal coordination control methods has mostly focused on arterial roads that carry uninterrupted traffic flow, and straight traffic flow has mainly been studied. In such cases, the through-flow movement is considered to be the highest proportion of traffic, while the turning flow accounts for a small proportion of traffic.

In the past, the key design objective of two-way signal progression has been to maximize traffic progression. Some scholars have put forward the MAXBAND model by considering the influence of left-turn traffic flow and initial queues [1–5]. However, due to differences in the characteristics of road sections, using various green bands in different road sections, to a certain extent, can increase the effect of traffic on the arterial road. Hence, the MULTIMAND model has been proposed [6–9]. To remove the symmetry restriction of the center line of the green band in the MULTIBAND model, Zhang et al. proposed the AM-BAND model [10].

Because two-way progression only considers through traffic flow, it has the following limitations: For arterial roads at connection points between urban traffic networks (such as the connection point between an urban expressway ramp and an arterial road), many vehicles may merge onto the arterial road at the connection point or drive out to other sections, and therefore, the turning traffic flow may be more than the through traffic flow. Therefore, traditional methods may lead to an imbalance between the traffic demand of the turning traffic flow and the obtained signal resources, and thus, conduct a second queue of turning traffic flow or even queue overflow.

Since the above methods only consider through traffic flow, the green bandwidth allocated to turning traffic flow is small, resulting in stop delay and queuing. Queue overflow also affects traffic efficiency in other directions. To address the above-mentioned problems, some scholars have put forward the concept of multi-path progression for arterial signal optimization. Yang (2015) defined the problem as a "multi-path progression model for synchronization of arterial traffic" [11], Chen (2021) defined it as an "arterial signal progression plan for multi-path flows" [12], and Li defined it as "multi-path arterial progression" [13]. The research objective is "multi-path signal progression" and the research scenario is "arterial traffic".

Multi-path signal progression provides multi-path travel belts both for through and turning path flows with significant traffic. Arsava et al. established the OD-NETBAND model which considered the origin and destination (OD) of the arterial vehicle paths and optimized the bandwidth according to OD data [14]. Lin et al. put forward the INTEBAND model (comprehensive green band model), which ensured the formation of variable green bands and coordinated the operation of social and public transport vehicles on the arterial [15]. However, the accuracy of the existing sensors needed to be improved, and the OD data were challenging to obtain. Based on this, Chen (2021) [12] used left-turn counting data, which were easier to obtain, to ensure the effectiveness of the green band and to overcome data acquisition difficulties by disassembling the path into a combination of multiple local bands. However, the assumptions of a path traffic calculation model can lead to deviations between calculated and actual traffic.

Figure 1 shows such an example of the Tianyuan West Road in Nanjing, which gives the change of traffic flow from 7 a.m. to 9 p.m. The flow of each path fluctuates throughout the day. The traffic flow in a multi-path model takes a value at a certain time, or the average over a period of time, and leads to the following two limitations:

- The above study does not consider the uncertainty of traffic flow. The model is significantly affected by changes in traffic flow, and the green bandwidth in the model is sensitive to changes in traffic flow.
- The optimized signal scheme in the model can only adapt to a certain traffic scenario. If it needs to be extended to multiple scenarios, the coordination control strategy needs to be changed according to the time-varying traffic. If the switching frequency of the signal scheme is low, it delays the current traffic demand; if it is high, it results in a heavy burden for drivers and increases the cost of traffic control.

For multiple uncertain traffic scenarios in a period of time, the existing timing signal control method generally uses the average or maximum value of traffic flow in a sampling period as the data input. It is widely used in engineering practice due to its simple calculations. However, only taking the average and maximum traffic flow in a period of time as the model input has the following limitations:

- With respect to average flow [16–18], this method uses the average value of all traffic flow samples in a sampling interval as the data input. Heydecker (1987) pointed out that if the variability of traffic flow was significant as compared with the timing obtained by considering this variability, optimizing signal timing relative to average flow could cause considerable additional delays [19]. For small variability, using average traffic flow in traditional calculation methods only results in a small loss of average performance (efficiency). It can be seen that the model is significantly affected by the volatility of traffic data, and it is difficult to represent the overall performance of traffic flow in a period of time only by taking the average value as the data input.
- Regarding maximum flow [20,21], This method selects the maximum value of all traffic flow samples in a sampling interval as the data input. Obviously, this method takes the time of maximum system load (maximum flow) as the research object. If the observation value of the highest flow is used, the solution of the model may be too conservative. More green light time may be allocated to the worst case of the system, resulting in a waste of the average performance (efficiency).

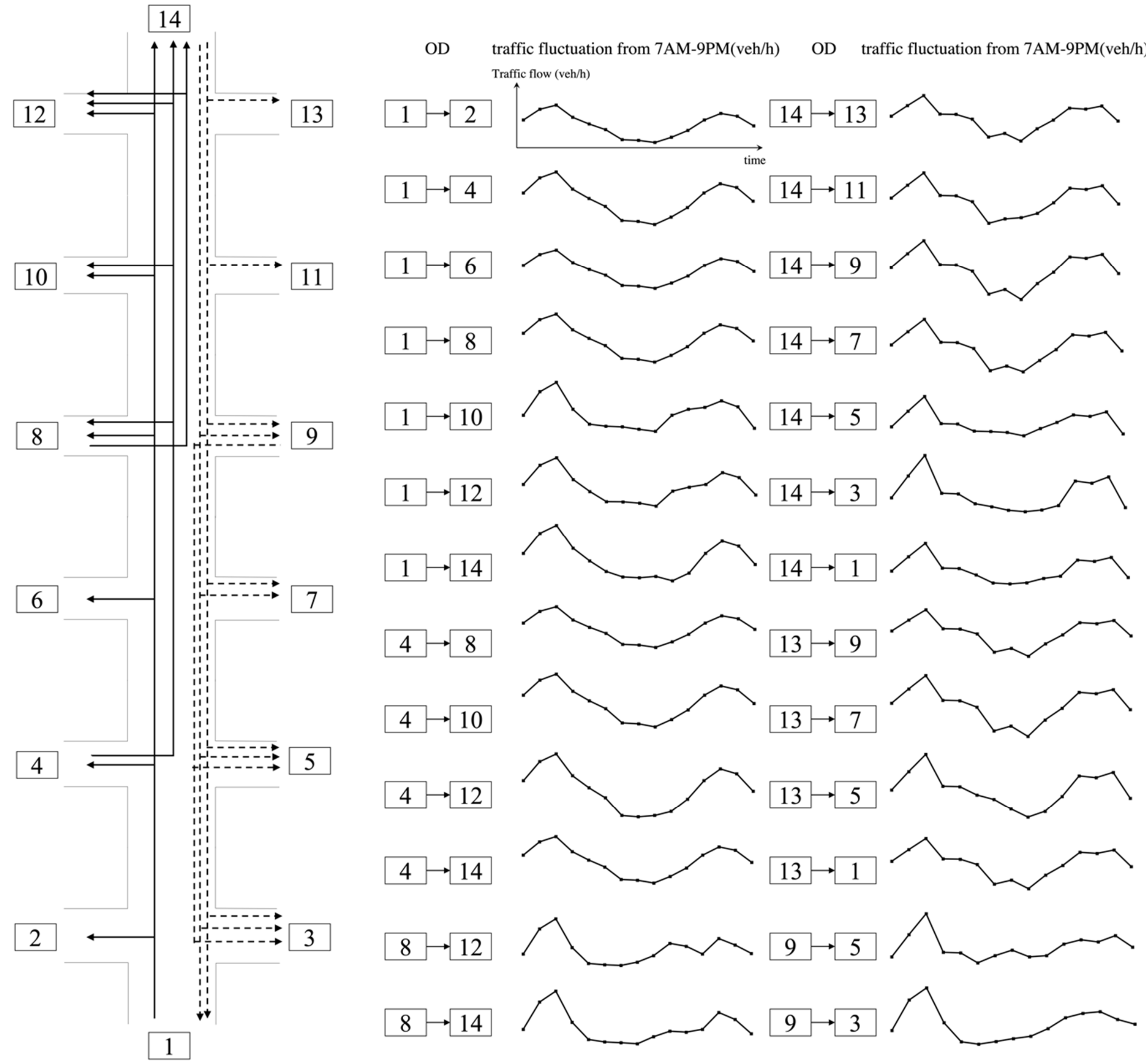

Figure 1. Flow fluctuations of different paths.

To address the above issues, we propose a model that represents the uncertainty of traffic flows via a limited number of discrete flow scenarios associated with the strictly positive probability of occurrence. Then, we attempt to optimize signal timing across these scenarios for near-optimal and stable solutions concerning a population of all possible realizations of uncertainty. Since the objective function is non-convex and non differentiable, we use a genetic algorithm (GA) to search for an optimum approximation solution. In addition, we apply a sensitivity analysis and obtain a weight factor that results in optimal model stability. The main contribution of this model is that decision-makers can choose the efficiency or stability of the model according to their preferences. To validate the results, we use the SUMO traffic simulation software to build the research area with traffic flow settings in each scenario. We change the signal plan according to the GA result. By monitoring the changing path flow delay, stop, and speed, we find that the GA result performs better than the spinal plan solved by the traditional MAXBAND method.

The remainder of this paper is organized as follows: The specific issues studied are described in Section 2. The proposed methodology is presented in Section 3. In Section 4, a case study and a simulation-based comparison experiment are presented to prove the effectiveness of the proposed model. In Section 5, sensitivity analyses are conducted to explore the influence of parameter variation on the model. Finally, we state the conclusions of this study in Section 6.

2. Problem Formulation

In this study, for the design of a new model to contend with multi-path arterial traffic patterns, we start with an investigation of the fundamental concept of two-way progression.

2.1. Two-Way Progression Model

The MAXBAND model [2] (Little, 1966) is a traditional signal coordination optimization method that considers the weighted bandwidth of the bidirectional progressive band. This model produces cycle time, offsets, speeds, and order of left-turn phases to maximize the weighted combination of bandwidths. The key model formulations are as follows:

$$Max\left(b + k\overline{b}\right) \tag{1}$$

The objective function of MAXBAND is to maximize the weighted sum of bidirectional bandwidth; $b\left(\overline{b}\right)$ is the green bandwidth for outbound (inbound) path i.

$$(1-\rho)\overline{b} \geq (1-\rho)\rho b \tag{2}$$

where ρ indicates the preference for inbound or outbound paths. Equation (2) allocates the progression preference to either the inbound or outbound direction.

$$\frac{1}{C_{max}} \leq c \leq \frac{1}{C_{min}} \tag{3}$$

where $C_{\min}(C_{max})$ is the boundaries of the cycle length and c is a decision variable that indicates the reciprocal of the cycle length. Equation (3) specifies the maximum and minimum values of the cycle.

$$w_i + b \leq 1 - r_i \qquad \forall i = 1, \ldots, n \tag{4}$$

$$\overline{w}_i + \overline{b} \leq 1 - \overline{r}_i \qquad \forall i = 1, \ldots, n \tag{5}$$

where $w_i(\overline{w}_i)$ is the duration before (after) the green bands for outbound (inbound) path i at intersection k, and r_i is the red time at path i. Equations (4) and (5) limit the green bandwidth within the available green time.

$$\begin{aligned} &(w_i + \overline{w}_i) - (w_{i+1} + \overline{w}_{i+1}) + \left(t_i + \overline{t}_i\right) + \delta_i L_i - \overline{\delta}_i \overline{L}_i - m_i \\ &= (r_{i+1} - r_i) + (\tau_i + \overline{\tau}_i) + \delta_{i+1} L_{i+1} - \overline{\delta}_{i+1} \overline{L}_{i+1} \; \forall i = 1, \ldots, n-1 \end{aligned} \tag{6}$$

where $L_i\left(\overline{L}_i\right)$ is the green time assigned to outbound (inbound) left-turning vehicles, $\tau_i(\overline{\tau}_i)$ is the decision variable that indicates the outbound (inbound) prevailing speed, and $\delta_i\left(\overline{\delta}_i\right)$, m_i is the integer variable that ensures that traffic flow is continuous during the green time.

$$c\left(\frac{d_i}{v_{max,i}}\right) \leq t_i \leq c\left(\frac{d_i}{v_{min,i}}\right) \forall i = 1, \ldots, n-1 \tag{7}$$

$$c\left(\frac{\overline{d}_i}{\overline{v}_{max,i}}\right) \leq \overline{t}_i \leq c\left(\frac{\overline{d}_i}{\overline{v}_{min,i}}\right) \forall i = 1, \ldots, n-1 \tag{8}$$

$$c\left(\frac{d_i}{\Delta v_{max,i}}\right) \leq \left(\frac{d_i}{d_{i+1}}\right) t_{i+1} - t_i \leq c\left(\frac{d_i}{\Delta v_{min,i}}\right) \forall i = 1, \ldots, n-2 \tag{9}$$

$$c\left(\frac{\overline{d}_i}{\Delta \overline{v}_{max,i}}\right) \leq \left(\frac{\overline{d}_i}{\overline{d}_{i+1}}\right) \overline{t}_{i+1} - \overline{t}_i \leq c\left(\frac{\overline{d}_i}{\Delta \overline{v}_{min,i}}\right) \forall i = 1, \ldots, n-2 \tag{10}$$

where $v_{min,i}$ and $v_{max,i}(\overline{v}_{min,i},\ \overline{v}_{max,i})$ are the minimum and maximum values for the outbound (inbound) speed, respectively; $\Delta v_{min,i}$ and $\Delta v_{max,i}$ $(\Delta\overline{v}_{min,i},\ \Delta\overline{v}_{max,i})$ are the minimum and maximum values for the outbound (inbound) speed change, respectively; $b,\ \overline{b},\ c, w_i, \overline{w}_i, t_i, \overline{t}_i \geq\ 0,\ \forall i = 1, \ldots, n$; m_i is an integer; $\delta_i,\ \overline{\delta}_i$ are binary integers, $\forall i = 1, \ldots, n$. The key variables in the model by Little et al. (1981) are shown in Figure 2.

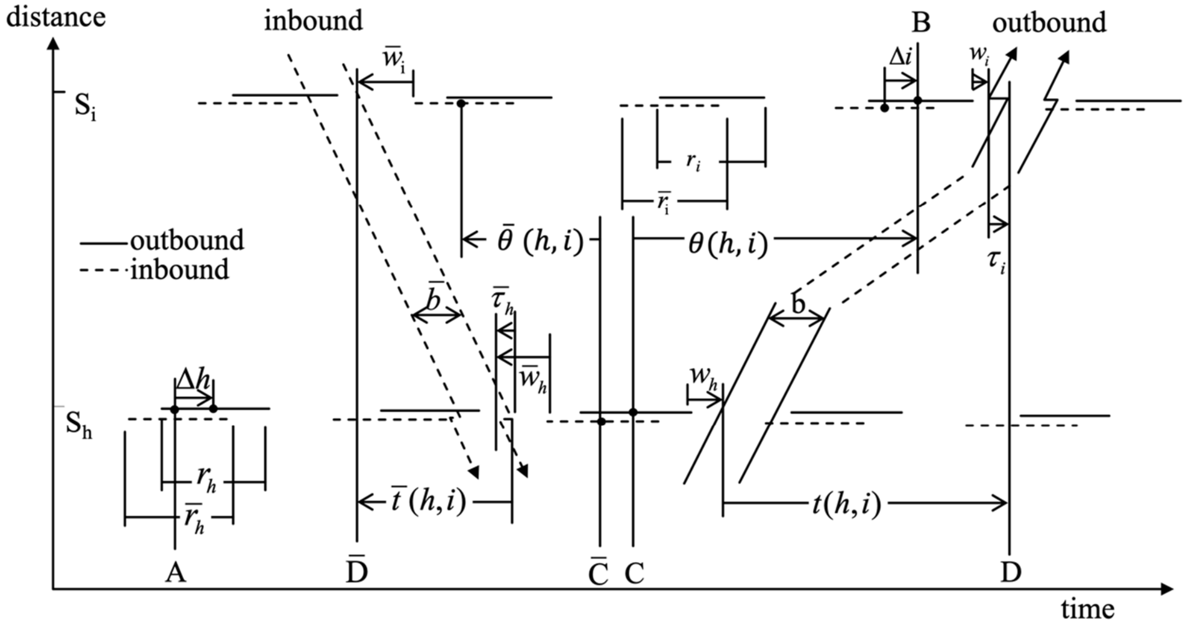

Figure 2. Bidirectional coordination optimization model based on MAXBAND (Morgan and Little, 1964).

2.2. Key Research Points of Multi-Path Progression

The traditional MAXBAND model is similar to sizeable two-way arterial traffic flow. This model allocates the largest signal resources to the traffic flow in the main direction without considering the traffic flow in the second direction, which may lead to unbalanced allocation of traffic flow resources in the second direction and queue overflow.

We define local path p as the inflow at the upstream intersection and the outflow at the downstream intersection. As shown in Figure 3, there are three turns at each intersection (TH, LT, and RT); therefore, 24 paths can be formed for outbound. Similarly, there are 24 paths in the opposite direction (inbound).

When coordinating arterial traffic signals, it is necessary to consider the coordination and allocation of multi-path signal resources. In this study, we need to solve the following key issues:

(1) Consider the uncertainty of traffic flow

A traditional timing control system carries out signal control according to a preset timing scheme without considering real-time vehicle information. It cannot adapt to changes in traffic flow. The system mainly considers traffic flow fluctuations in a day, divides the day into several periods, and calculates the time allocation according to the average flow of each period. However, traffic flow also fluctuates significantly in the same period. If only the fixed flow is used as the basis for timing, then, the timing scheme will be sensitive to flow fluctuations and will have poor stability.

Therefore, the model should balance efficiency and stability simultaneously and should provide a signal scheme compatible with more scenarios (improve the scheme's stability) under the condition that delay and traffic efficiency can be accepted.

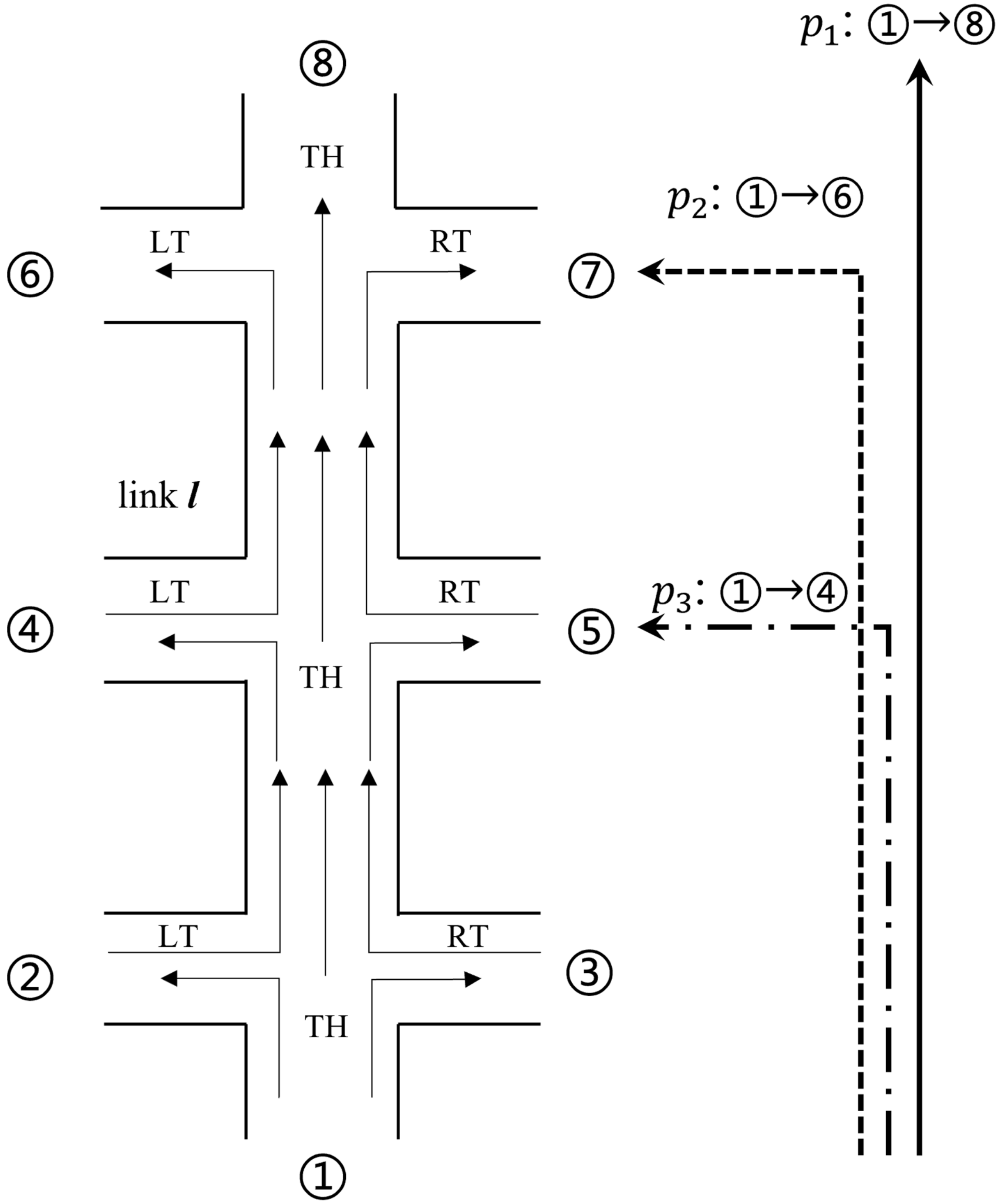

Figure 3. Upstream inflows and downstream outflows form a path.

(2) Consider the collaborative optimization of multiple path bandwidth, rather than only the arterial direction

According to the MAXBAND model, the objective function is to maximize the bandwidth of p_1 and its opposite direction path. The result is that when green time is allocated, the through phase of each intersection receives more signal resources. It is worth noting that if the left-turn flow at the downstream intersection accounts for a large proportion (p_2, p_3), the MAXBAND model results in less green time allocated to the left-turn flow. As shown in Figure 4, under uneven signal resource allocation, two scenarios of left-turn and through traffic flow congestion seriously affect traffic efficiency.

(3) Concurrently optimizing the signal phase sequence and offsets

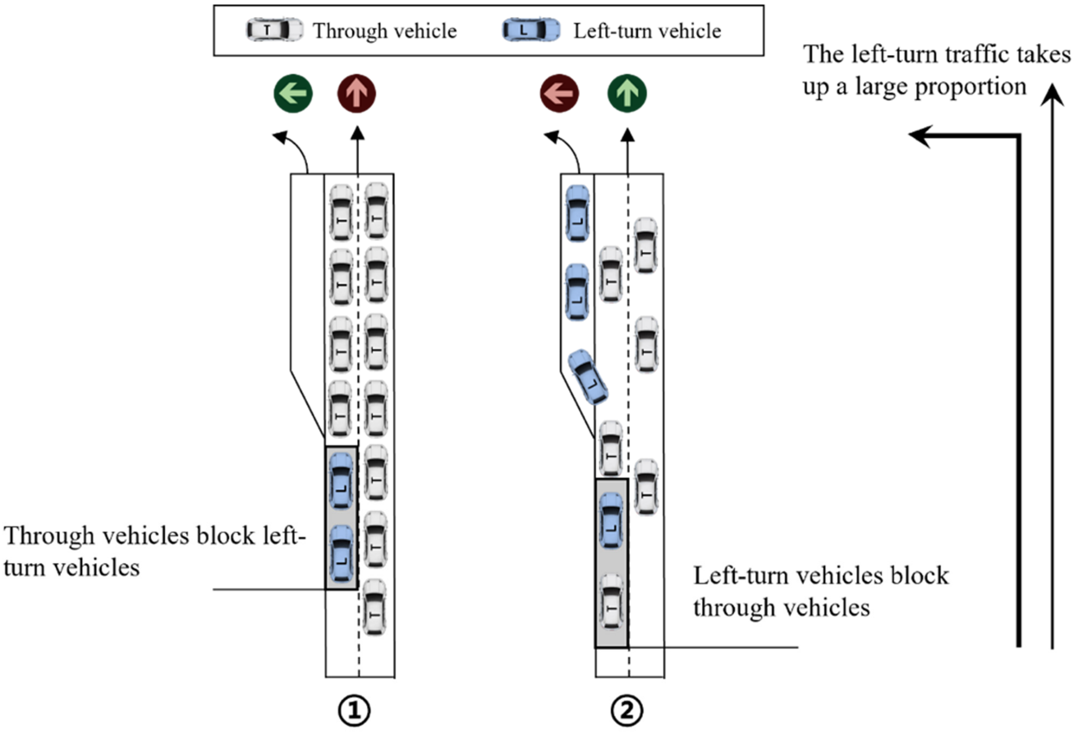

Figure 4. Considering only through vehicles causes queuing congestion.

As shown in Figure 5, after adjusting the phase sequence and offset of three intersections, the green wave band b_2 is significantly more comprehensive, and the bandwidth b_1 becomes zero. We can conclude that each path's bandwidth is affected by the phase sequence and offset, and therefore, we need to consider optimizing the phase sequence and offset in the model to improve the overall weighted bandwidth.

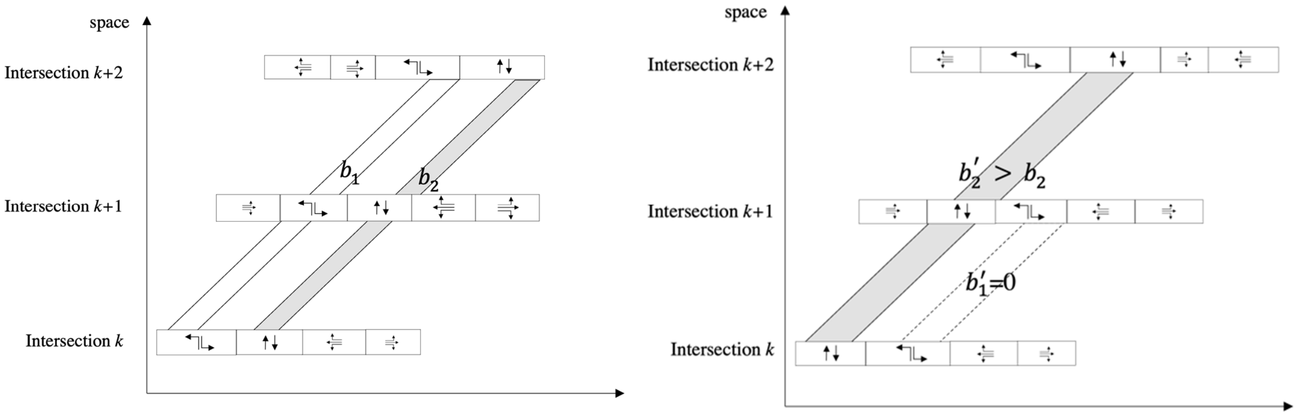

(**a**) (**b**)

Figure 5. Demonstration of the change of bandwidth after optimized phase sequence and offset: (**a**) The bandwidth under the original phase sequence; (**b**) the bandwidth after changing the phase sequence.

3. Methodology

In this section, we introduce the multi-path control model considering traffic flow uncertainty. This model is based on the MAXBAND model, considers the optimization of phase sequence and offset, and then maximizes the weighted bandwidth of all paths in multiple traffic scenarios. The key symbols in the model are explained in Table 1.

Table 1. Symbol interpretation.

Symbol	Description
$\varphi_i(\overline{\varphi}_i)$	The weighting factor for the outbound (inbound) path i
$f_i(\overline{f}_i)$	The flow for the outbound (inbound) path i (veh/h)
$g_{i,k}\left(\overline{g}_{i,k}\right)$	The green duration that the outbound (inbound) path i can obtain at intersection (s)
$x_{i,m,k}$	The dummy variable, $x_{i,m,k} = 1$ indicates that the phase m of path i at intersection k is green
$T_{m,k}$	The duration of phase m at intersection k (s)
$y_{m,n,k}$	The dummy variable, $y_{m,n,k} = 1$ indicates that the phase m is before phase n in the same cycle of intersection k
θ_k	The offset of intersection k (s)
$r_{i,k}\left(\overline{r}_{i,k}\right)$	The red duration at the left(right) side of the green bands for path i (s)
$t_k\left(\overline{t}_k\right)$	The travel time between intersection k and downstream intersection (s)
$n_{i,k}\left(\overline{n}_{i,k}\right)$	The integer variables represent the number of cycles
$\tau_{i,k}\left(\overline{\tau}_{i,k}\right)$	The initial queue cleaning time at intersection k of path i (s)
π_k	The occurrence probability of scenario k
γ	The weight coefficient
$P(\overline{P})$	The set of outbound (inbound) paths
I_i	The set of intersections passed by the path i
M	A large positive number, which can keep the inequality true when phase m in the path i is not green
S	The set of the traffic situation

Based on the MAXBADN model and considering two-way multi-path coordination control, the following models can be proposed:

$$
\begin{aligned}
Obj:\ Max\Bigg\{ & \gamma\left(\sum_i\sum_k \pi_i^a\varphi_i b_i + \sum_i\sum_k \pi_i^a\overline{\varphi}_i\overline{b}_i\right) \\
& -(1-r)\sqrt{\sum_i\sum_k \pi_i^a\left[\left(\varphi_i b_i + \overline{\varphi}_i\overline{b}_i\right) - \left(\sum_i\sum_k \pi_i^a\varphi_i b_i + \sum_i\sum_k \pi_i^a\overline{\varphi}_i\overline{b}_i\right)\right]}\Bigg\}
\end{aligned}
$$

$$
s.t.\begin{cases}
\varphi_i = \frac{f_i}{\sum_i f_i} \\
\overline{\varphi}_i = \frac{\overline{f}_i}{\sum_i \overline{f}_i} \\
0 \le w_{i,k} + b_i \le \sum\limits_l g_{i,k}\ \forall i \in P; \forall k \in I_i \\
0 \le \overline{w}_{i,k} + \overline{b}_i \le \sum\limits_l \overline{g}_{i,k}\ \forall i \in \overline{P}; \forall k \in I_i \\
g_{i,k} = \beta_{i,m,k}T_{m,k}\ \forall i \in P; \forall k \in \sigma_i \\
\overline{g}_{i,k} = \beta_{i,m,k}T_{m,k}\ \forall i \in \overline{P}; \forall k \in \sigma_i \\
y_{m,m,k} = 0\ \forall m; \forall k \in I_i \\
y_{m,n,k} + y_{n,m,k} = 1\ \forall m \ne n; \forall k \in I_i \\
y_{m,n,k} \ge y_{m,n,k} + y_{n,n',k} - 1\ \forall m \ne n \ne n'; \forall k \in I_i \\
\theta_k + r_{i,k} + w_{i,k} + t_k + n_{i,k} = \theta_{k+1} + r_{i,k+1} + w_{i,k+1} + \tau_{i,k+1} + n_{i,k+1}\ \forall i \in P; \forall k \in I_i \\
\overline{n}_{i,k} + \overline{w}_{i,k} + \overline{r}_{i,k+\overline{t}_k} - \overline{\tau}_{i,k} \pm \theta_k = \overline{r}_{i,k+1} + \overline{w}_{i,k+1} + \overline{n}_{i,k+1} - \theta_{k+1}\ \forall i \in \overline{P}; \forall k \in I_i \\
r_{i,k} \le \sum\limits_m x_{i,m,k}y_{m,n,k}\cdot T_{m,k} + M(1 - x_{i,m,k})\ \forall i \in P + \overline{P}; \forall k \in I_i; \forall n \\
\overline{r}_{i,k} \le \sum\limits_m x_{i,m,k}y_{n,m,k}\cdot T_{m,k} + M(1 - x_{i,m,k})\ \forall i \in P + \overline{P}; \forall k \in I_i; \forall n \\
r_{i,k} + \overline{r}_{i,k} + \sum\limits_m x_{i,m,k}\cdot T_{i,k} = 1\ \forall i \in P + \overline{P}; \forall k \in I_i \\
x_{i,m,k} = \begin{cases} 1, \text{ if phase } m \text{ of path } i \text{ at intersection } k \text{ is green;} \\ 0, \text{ o. w.} \end{cases} \\
y_{m,n,k} = \begin{cases} 1, \text{ if phase } m \text{ is before phase } n \text{ in the same cycle of intersection } k; \\ 0, \text{ o. w.} \end{cases} \\
b_i, w_{i,k}, \overline{b}_i, \overline{w}_{i,k} \ge 0\ \forall i \in P + \overline{P}; \forall k \in I_i
\end{cases}
$$

Based on MAXBAND, the weighted bandwidth of bidirectional multi-path is considered in Equation (11):

$$Max \sum_i (\varphi_i b_i) + \sum_i \left(\overline{\varphi}_i \overline{b}_i\right) \tag{11}$$

$$\varphi_i = \frac{f_i}{\sum_i f_i} \tag{12}$$

$$\overline{\varphi}_i = \frac{\overline{f}_i}{\sum_i \overline{f}_i} \tag{13}$$

where $\varphi_i(\overline{\varphi}_i)$ is the weighting factor for the outbound (inbound) path i; $f_i(\overline{f}_i)$ is the flow for the outbound (inbound) path i. Equations (12) and (13) indicate that the weighting factor of path bandwidth is proportional to the path. For paths with large traffic, more signal resources should be allocated:

$$0 \leq b_i + w_{i,k} \leq g_{i,k} \ \forall i \in P; \forall k \in I_i \tag{14}$$

$$0 \leq \overline{b}_i + \overline{w}_{i,k} \leq \overline{g}_{i,k} \ \forall i \in \overline{P}; \forall k \in I_i \tag{15}$$

where $g_{i,k} \left(\overline{g}_{i,k}\right)$ is the green duration that the outbound (inbound) path i can obtain at intersection k (calculated by predetermined phase sequences), $P\left(\overline{P}\right)$ is the set of outbound (inbound) paths, and I_i is the set of intersection passed by the path i. Equations (14) and (15) are the interference constraints.

To describe the signal phases of different paths, define $x_{i,m,k}$ as a dummy variable, $x_{i,m,k} = 1$ indicates that the phase m of path i at intersection k is green, otherwise, $x_{i,m,k} = 0$. Therefore, the green duration $g_{i,k}$ can be expressed as follows:

$$g_{i,k} = x_{i,m,k} \cdot T_{j,k} \qquad \forall i \in P; \forall k \in I_i \tag{16}$$

$$\overline{g}_{i,k} = x_{i,m,k} \cdot T_{j,k} \qquad \forall i \in \overline{P}; \forall k \in I_i \tag{17}$$

where $T_{m,k}$ is the duration of phase m at intersection k. Then, the interference constraints can be re-expressed as follows:

$$0 \leq w_{i,k} + b_i \leq \sum_m x_{i,m,k} \cdot T_{m,k} \ \ \forall i \in P; \forall k \in I_i \tag{18}$$

$$0 \leq \overline{w}_{i,k} + \overline{b}_i \leq \sum_m x_{i,m,k} \cdot T_{m,k} \ \ \forall i \in \overline{P}; \forall k \in I_i \tag{19}$$

Similarly, to optimize the signal phase sequence, define $y_{m,n,k}$ as the dummy variable representing the phase sequence; $y_{m,n,k} = 1$ indicates that the phase m is before phase n in the same cycle of intersection k, otherwise $y_{m,n,k} = 0$.

To ensure the correctness and solvability of phase sequence in time sequence, the time constraints of phase sequence at intersections are as follows:

$$y_{m,n,k} + y_{n,m,k} = 1 \ \ \forall m \neq n; \forall k \in I_i \tag{20}$$

$$y_{m,m,k} = 0 \ \ \forall m; \forall k \in I_i \tag{21}$$

Equations (20) and (21) indicate that the sequence of two adjacent phases is unique. To ensure that the phase sequence advances according to the complete cycle of the signal and to prevent local phase sequence cycles, the relationship between multiple phase sequences in a cycle can be expressed as follows:

$$y_{m,n',k} \geq y_{m,n,k} + y_{n,n',k} - 1 \ \ \forall m \neq n \neq n'; \forall k \in I_i \tag{22}$$

Equation (22) indicates that if phase m is before phase n ($x_{m,n,k}$ = 1) and phase n is before phase n', then phase m is before phase n' ($m \to n \to n'$).

When considering multi-path progress with time cycle constraints, we can substitute Equation (6) in the MAXBAND model into multi-path. In addition, it is also necessary to consider that integer loop constraints in the original model may lead to invalid bandwidth for some paths. The time cycle constraints of multi-path improvement are given as follows (the progress of outbound green bands from point ① to point ② of Figure 6):

$$\begin{gathered} \theta_k + r_{i,k} + w_{i,k} + t_k + n_{i,k} = \theta_{k+1} + r_{i,k+1} + w_{i,k+1} + \tau_{i,k+1} + n_{i,k+1} \\ \forall i \in P; \forall k \in I_i \end{gathered} \tag{23}$$

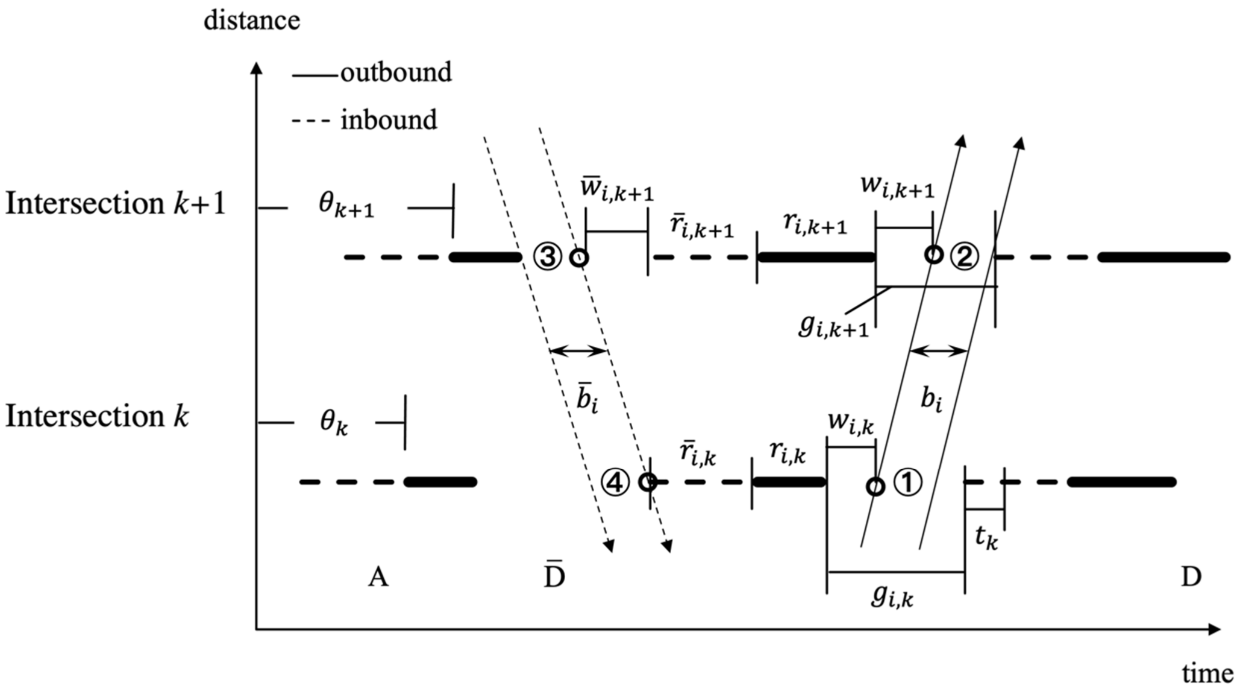

Figure 6. Explanation of key variables.

Similarly, we can obtain the time cycle constraints of the reverse path as follows (the progress of an outbound green band from point ③ to point ④ of Figure 6):

$$\begin{gathered} \bar{n}_{i,k} + \bar{w}_{i,k} + \bar{r}_{i,k+\bar{t}_k} - \bar{\tau}_{i,k} - \theta_k = \bar{r}_{i,k+1} + \bar{w}_{i,k+1} + \bar{n}_{i,k+1} - \theta_{k+1} \\ \forall i \in \bar{P}; \forall k \in I_i \end{gathered} \tag{24}$$

where θ_k is the offset of intersection k, $r_{i,k}(\bar{r}_{i,k})$ is the red duration at the left (right) side of the green band for path i (calculated by predetermined phase sequences), $t_k(\bar{t}_k)$ is the travel time between intersection k and downstream (upstream) intersection, $n_{i,k}(\bar{n}_{i,k})$ is the integer variables which represent the number of cycles, $\tau_{i,k}(\bar{\tau}_{i,k})$ is the initial queue cleaning time at intersection k of path i.

The MAXBAND model applies to the scenario where the signal phase sequence and offset are given. However, when we optimize the overall signal scheme by changing the phase sequence, the red duration of path i before (after) its available green time ($r_{i,k}$) becomes a non-fixed value and is affected by the change in the phase sequence. Therefore, the relationship between the phase sequence and $r_{i,k}$ is given as follows:

$$r_{i,k} \leq \sum_m x_{i,m,k} y_{m,n,k} \cdot T_{m,k} + M(1 - x_{i,m,k}) \;\; \forall i \in P + \bar{P};\; \forall k \in I_i;\; \forall n \tag{25}$$

$$\bar{r}_{i,k} \le \sum_m x_{i,m,k} y_{n,m,k} \cdot T_{m,k} + M(1 - x_{i,m,k}) \;\; \forall i \in P + \overline{P};\; \forall k \in I_i;\; \forall n \tag{26}$$

$$r_{i,k} + \bar{r}_{i,k} + \sum_m x_{i,m,k} \cdot T_{i,k} = 1 \;\; \forall i \in P + \overline{P};\; \forall k \in I_i \tag{27}$$

where M is a large positive number, which can keep the inequality true and dominate other variables when phase m in path i is not green ($x_{i,m,k} = 0$).

Since path i may receive green in multiple consecutive phases, Equations (25) and (26) ensure that $r_{i,k}(\bar{r}_{i,k})$ is taking place prior (after) to the first (last) phase that is given green to path i, Equation (25) ensures that $r_{i,k}$ is connected before the first phase of path i, Equation (26) ensures that $r_{i,k}$ is connected after the last phase of path i, Equation (27) is the total green duration in a cycle of path i.

To ensure that the signal scheme can map multiple flow distribution intervals in practical applications and to reduce the sensitivity of the signal scheme to changes in flow, in this study, we propose the following control methods to adapt to traffic fluctuations.

This study is based on the multi-scenario method, where scenarios represent possible traffic conditions. In a scenario, each approach's traffic volume and other parameters are constant. The principle of this method is to express the fluctuation of traffic flow as a finite number of discrete traffic scenarios, k, and their occurrence probability, π_k, to form the traffic scenario set S.

The average bandwidth in different scenarios is used to represent the efficiency of the control model, and the standard deviation is used to represent the stability of the control model. The average-standard (Shapiro, A. et al., 2009 [22]) deviation model (MSD) changes the preference for efficiency and stability by adjusting the efficiency-stability weight. The objective function can be expressed as:

$$\begin{aligned} Max\Bigg\{ &\gamma\left(\sum_i\sum_k \pi_i^a \varphi_i b_i + \sum_i\sum_k \pi_i^a \overline{\varphi}_i \overline{b}_i\right) \\ &-(1-\gamma)\sqrt{\sum_i\sum_k \pi_i^a\left[\left(\varphi_i b_i + \overline{\varphi}_i \overline{b}_i\right) - \left(\sum_i\sum_k \pi_i^a \varphi_i b_i + \sum_i\sum_k \pi_i^a \overline{\varphi}_i \overline{b}_i\right)\right]}\Bigg\} \end{aligned} \tag{28}$$

where a is a scenario in the scenario set S; π_a is the occurrence probability of scenario a; γ is the efficiency-stability index ($0 \le \gamma \le 1$), the size of it depends on whether the decision-maker is more inclined to traffic efficiency (the weight of the green bandwidth) or stability (the sensitivity of the signal scheme). When $\gamma = 1$, it indicates that the uncertainty of traffic flow is not considered.

The objective function is continuous, and the feasibility set is nonempty, closed, and bounded. According to the Weierstrass theorem [23], there is an optimal solution to the optimization problem. However, because the objective function is non-convex and non-differentiable, it may be difficult to obtain the global optimum. The linear structure of the problem allows genetic algorithms to effectively solve local optimization problems. The genetic algorithm solution steps are as follows:

Step 1 Parameters are input, including intersection geometry and traffic flow distribution.

Step 2 According to the traffic demand distribution, the traffic scenario set S is randomly generated.

Step 3 The control scheme is generated based on a genetic algorithm, including initial population, roulette selection, binary crossover, inconsistent mutation, parent and offspring population merging.

Step 4 Fitness is calculated. The individual control scheme is run in each traffic scenario, and the individual fitness is calculated according to the objective function, and the top 50% of the optimal individuals are selected.

Step 5 For iterative termination condition judgment, if the improvement value of the two iterations is less than the set value, the iterative calculation is stopped, otherwise it is transferred to Step 3.

In this paper, the offset θ_k, phase sequence $\chi_{i,m,k}$, and integer cycle of each intersection $n_{i,k}$ are coded. To obtain the final solution of this problem, the offset θ_k; left and right red light duration r_{ik} and $r_{i,k}$, respectively; the green duration before (after) the green band $w_{i,k}$; and the integer cycle are used to draw the time-space diagram (Figure 6) of signal operation. The progression b_i can be easily calculated from the time-space diagram, and our goal is to maximum average bandwidth or the minimum bandwidth standard deviation.

Figure 7 shows the generation process uncertainty flow scenarios. In the first step, we generate hundreds of scenarios with uncertain traffic flow based on field survey data. For each traffic scenario, we obtain one intersection flow matrix. Since our goal is the multi-path progression, in the second step, the OD information of the multi-path is calculated according to the intersection flow matrix, and the uncertainty of intersection flow is converted into the uncertainty of the path flow, thus, we obtain the path traffic scenario matrix. Finally, the solution of the model is obtained through a genetic algorithm.

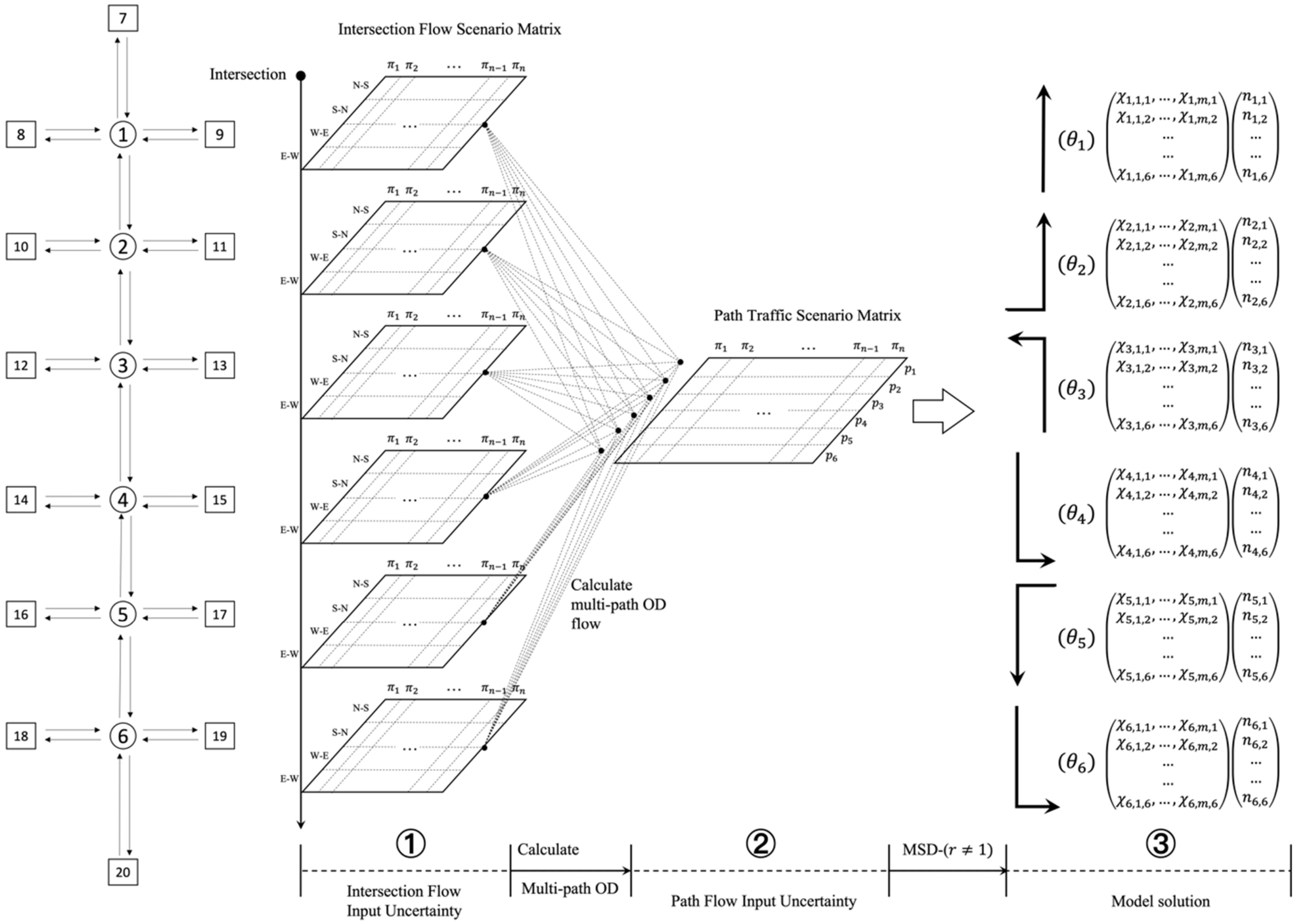

Figure 7. Uncertainty flow scenarios' generation framework.

4. Case Study

For this experiment, we select six intersections of Shuang Long Avenue in Nanjing as the research area. The distribution and connection status of the intersections are shown in Figure 8a, and the distribution of travel times between intersections is shown in Figure 8b. The travel times between intersections from Intersection 1 to 6 are 15 s, 40 s, 35 s, 23 s, and 25 s, respectively.

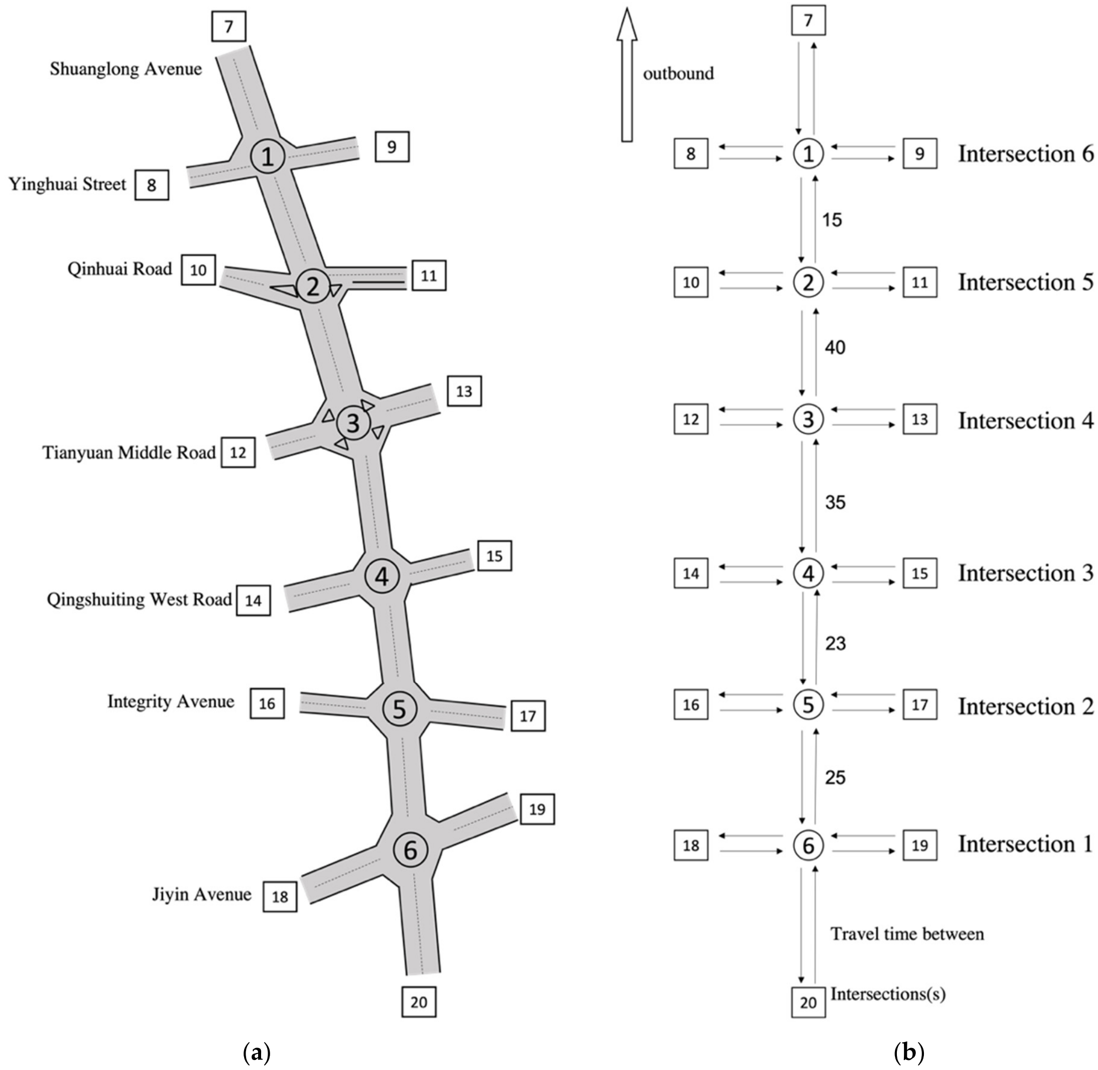

Figure 8. Intersections and travel time distribution.: (**a**) Distribution of experimental intersections; (**b**) intersection travel time distribution.

Figure 9 shows each intersection and node that the path passes through. Six paths are selected as the research object, and the OD nodes of the six paths are as follows: Path 1, 20→7; Path 2, 16→7; Path 3, 20→12; Path 4, 7→13; Path 5, 15→20; Paths 6, 7→17. The directions of Paths 1, 2, and 3 are outbound, and the directions of Paths 4, 5, and 6 are inbound.

Figure 10 shows the phase sequence and signal-to-time for the six intersections. The signal cycle of an intersection is 190 s; Intersections 1, 2, 3, and 5 have four-phase signal sequences; Intersections 4 and 6 have five-phase signal sequences. The values of other model parameters are as follows: Initial queue cleaning time $\tau_{i,k}(\overline{\tau}_{i,k}) = 3s$, population quantity = 500, maximal termination algebra = 1000, crossover probability = 0.5, and mutation probability = 0.01.

The more traffic scenarios considered, the closer to the true flow distribution in traffic scenarios. However, too many scenarios would increase the optimization model calculation speed. Mulvey et al. [24] conducted a detailed study on this and found that the ideal situation could be approached without listing excessive scenarios, and the number of scenarios a was equal to 200. Therefore, we selected 200 flow scenarios from the field data for the same time-of-day interval (sampling every 5 min from 6:00 a.m. to 10:40 p.m.) on Nanjing Shuang Long Avenue. Table 2 shows the average value, standard deviation, and maximum and minimum values of traffic volume of different approaches at each intersection. We assume that the probability of occurrence of these 200 scenarios is the same. The probability of occurrence of a certain value would be reflected by the frequency of occurrence in all scenarios.

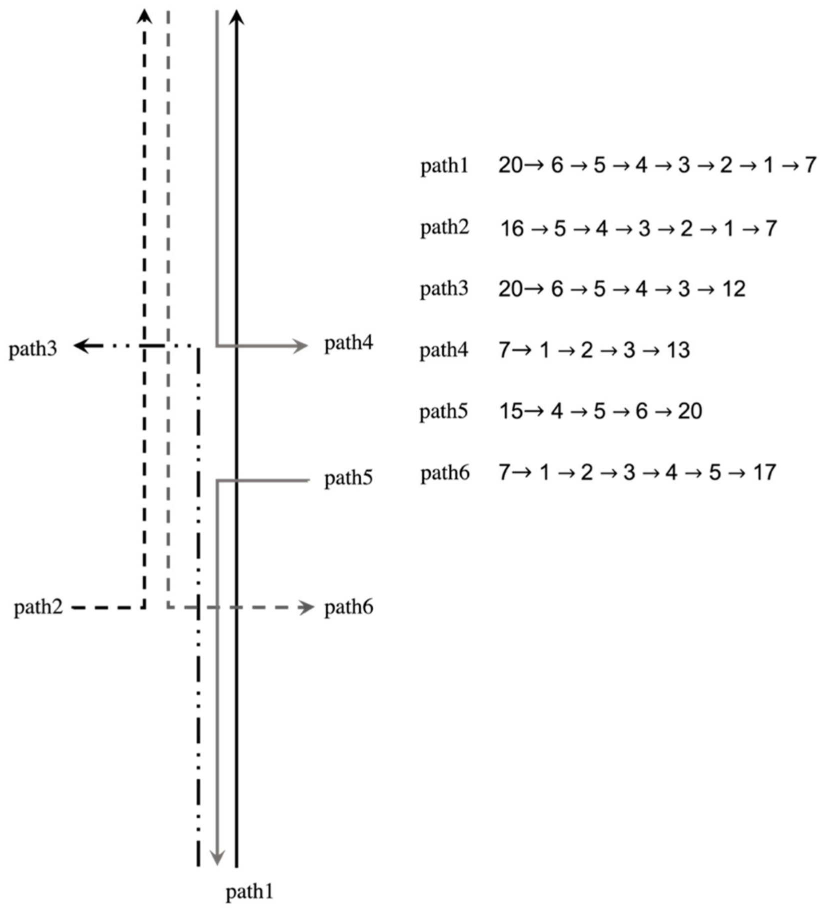

Figure 9. Critical path distribution.

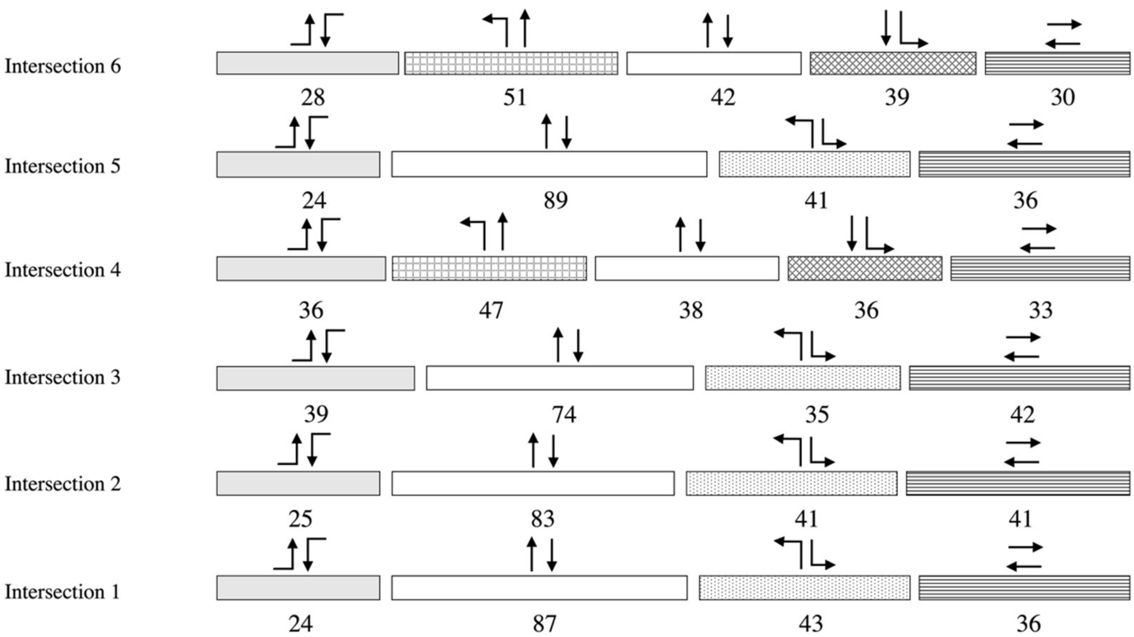

Figure 10. Intersection signal scheme.

Table 2. Intersection flow distribution.

Intersection		Intersection 1				Intersection 2				Intersection 3				Intersection 4				Intersection 5				Intersection 6			
Direction	**Turn**	**AVG**	**SD**	**MIN**	**MAX**	**AVG**	**SD**	**MIN**	**MAX**	**AVG**	**SD**	**MIN**	**MAX**	**AVG**	**SD**	**MIN**	**MAX**	**AVG**	**SD**	**MIN**	**MAX**	**AVG**	**SD**	**MIN**	**MAX**
N-S	LT	425	35	300	550	395	45	350	545	390	45	305	495	505	25	395	605	225	15	205	290	270	25	350	460
	TH	475	40	450	650	445	55	400	645	345	30	305	395	625	20	495	705	345	25	305	390	475	35	455	510
	RT	340	75	300	400	325	90	250	445	330	15	305	395	340	45	295	405	240	35	205	310	360	40	305	460
S-N	LT	305	25	250	400	435	45	350	595	340	25	210	445	545	50	445	755	345	60	205	440	440	55	400	560
	TH	410	25	350	450	465	25	450	495	390	40	315	495	475	35	445	555	415	75	305	495	460	15	400	560
	RT	345	15	300	400	395	85	300	445	370	45	325	395	440	40	295	655	415	35	305	490	280	20	255	310
W-E	LT	265	70	300	400	260	25	200	295	305	55	215	345	280	45	195	355	250	60	205	310	320	15	250	410
	TH	315	75	250	400	445	45	400	495	290	70	225	395	275	55	395	455	290	75	205	400	365	90	350	410
	RT	245	45	200	300	400	30	350	445	365	15	260	395	325	60	295	405	255	35	255	290	350	100	330	410
E-W	LT	345	60	200	450	265	50	200	345	400	25	275	345	275	75	245	405	365	20	305	440	270	25	200	310
	TH	365	35	300	450	390	45	350	495	290	45	250	345	385	20	345	555	285	45	255	440	390	45	320	460
	RT	255	45	200	300	315	90	250	395	310	20	260	345	380	25	295	455	345	25	255	410	400	20	300	510

Using the model proposed in this study, without considering the fluctuations of traffic flow ($r = 1$), take the average flow of each path as the input of the model, and obtain the temporal and spatial changes of the green wave under the consideration of traffic flow fluctuation, as shown in Figure 11, where the bandwidth of six paths is 11 s, 25 s, 22 s, 36 s, 39 s, and 41 s. Paths 4–6 have a larger bandwidth because downlink traffic accounts for a large proportion, and more signal resources are allocated.

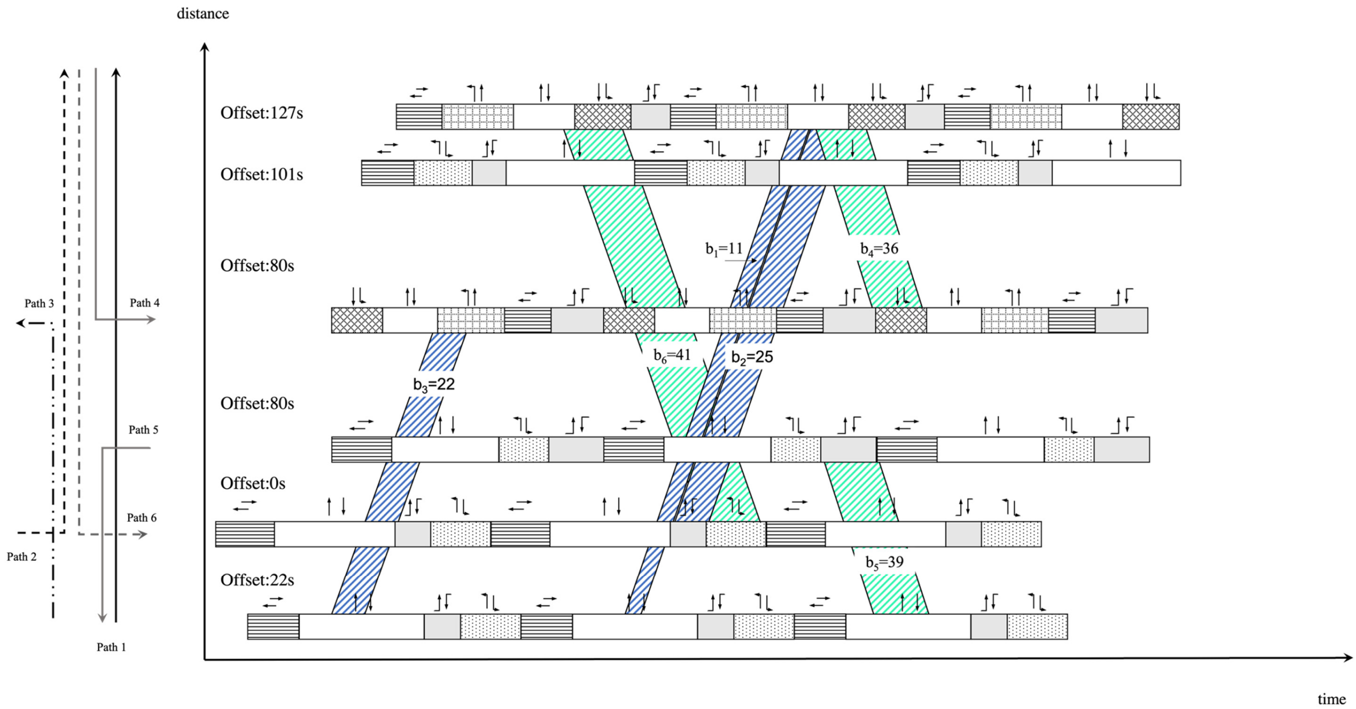

Figure 11. Spatial-temporal variation of green bands obtained by flow mean value (MSD-$r = 1$).

Considering fluctuations in traffic flow at each intersection, the efficiency-stability coefficient is taken to be 0.3 (it was proven, in the subsequent sensitivity analysis in this study, that when $r = 0.3$, the average bandwidth loss of each path is the minimum). The spatial-temporal change in the green wave under the scenario of considering traffic flow fluctuations is obtained and is shown in Figure 12, where the bandwidths of six paths are 13 s, 25 s, 22 s, 36 s, 39 s, and 39 s, and Paths 4–6 have larger bandwidths. Although the average traffic value of Path 4 is smaller than Path 3, it still gains greater weight. This is because the traffic fluctuation of Path 4 is slight, and the impact on stability is more significant than on efficiency, and therefore, more signal resources are allocated. As compared with $r = 1$, the bandwidth of Path 6 decreases, and the bandwidth of Path 1 increases, which is because the model focuses on the stability of bandwidth, and the volatility of traffic in Path 1 is large. Therefore, the bandwidth allocated is smaller than that, only considering the model's efficiency ($r = 1$). The bandwidths of Paths 2–5 stayed the same because they reached the maximum bandwidth in all phase sequence combination scenarios.

To evaluate the traffic operation of different models, SUMO [25] is selected as the simulation software in this study, with the model solution results as the simulation input, and the final output results are shown in Table 3. The changes in operating parameters of the three models in each path are shown in Figure 13.

The optimal mean value of each index appears in the MSD-$r = 1$ model, which shows the superiority of the multi-path model as compared with the basic MAXBAND model. As compared with the MSD-$r = 1$ model, the average performance of the MSD-$r = 0.3$ model has a certain degree of loss because the model is more inclined to consider the overall stability, and the sacrifice of operating efficiency is acceptable. From the perspective of the stability of each index, the optimal situation appears in the MSD-$r = 0.3$ model, which proves that the model has the most effective ability to resist the wave disturbance of traffic flow (the best stability). In addition, the MAXBAND and the MSD-$r = 1$ models only aim at efficiency (maximum green bandwidth), therefore, their stability performance is similar. Therefore, the MSD-$r = 0.3$ model performs well in the traffic flow fluctuation scenario, which can significantly improve the stability of the model on the premise of decreased efficiency loss.

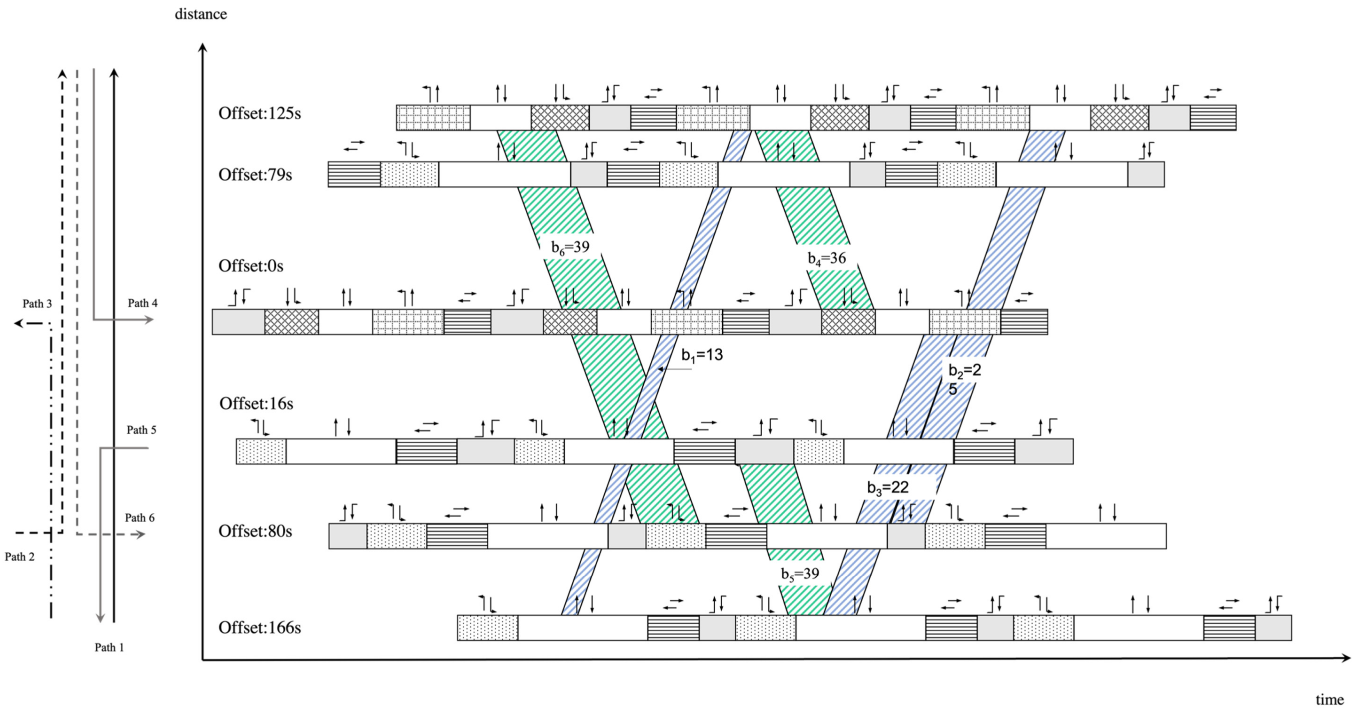

Figure 12. Spatial-temporal variation of green bands obtained by flow uncertainty (MSD-r = 0.3).

Table 3. Arterial performance under the control of different models.

Index		MAXBAND	MSD-r = 1	MSD-r = 0.3
Path-flow delay (s)	Average	69.80	63.94	66.10
	Standard deviation	13.29	11.20	6.06
	Maximum	143.25	128.67	111.68
Stops	Average	1.25	1.02	1.12
	Standard deviation	5.21	4.25	3.55
	Maximum	1.73	1.56	1.18
Speed (km/h)	Average	38.34	50.14	50.25
	Standard deviation	10.60	8.71	5.89
	Maximum	56.26	59.31	67.23

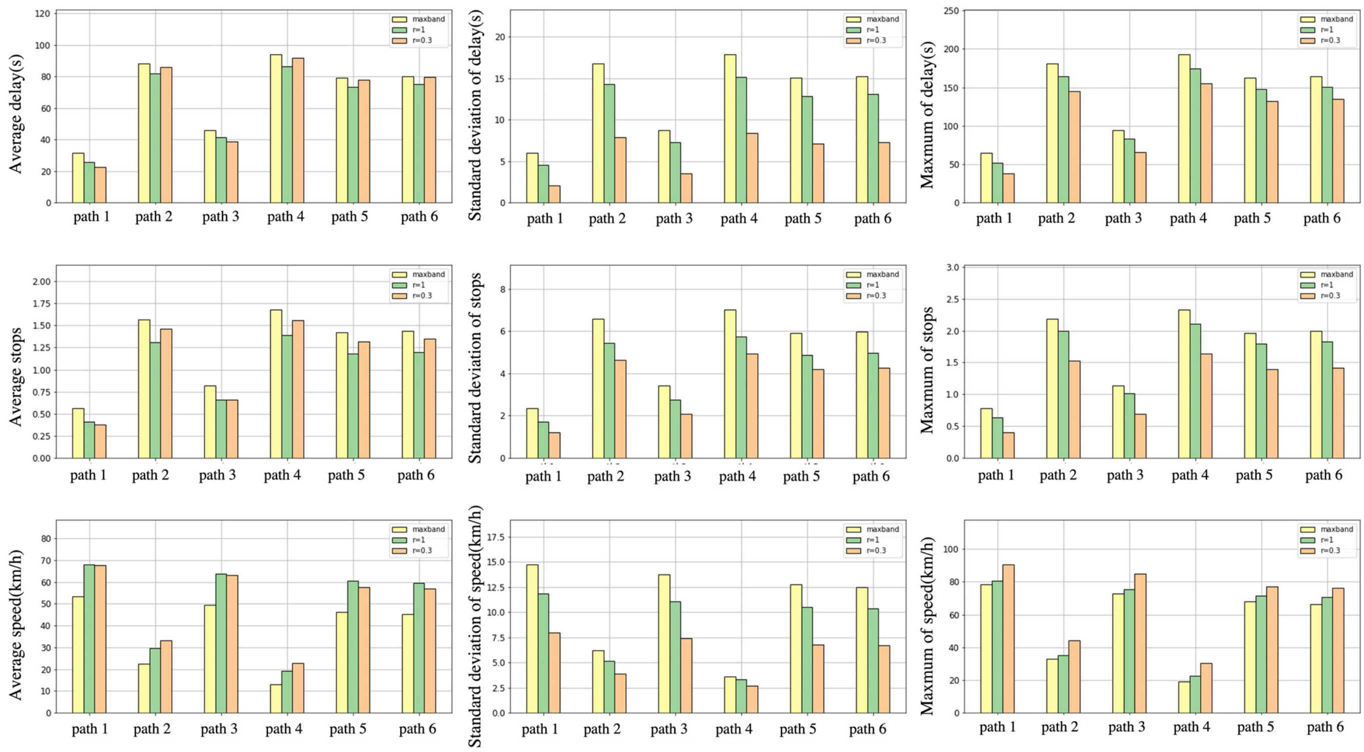

Figure 13. Operating parameters of each path.

5. Sensitivity Analyses

To further verify the applicability of the heuristic approach for the multi-path control method proposed in this study, in this section, we conduct a sensitivity analysis on the model's key parameters to explore the impact of the efficiency-stability coefficient value and traffic flow distribution on the model's performance. Except for the key variables, the values of traffic parameters are the same as those in the previous section. The settings for the sensitivity analysis experiments are shown in Table 4.

Table 4. Sensitivity analysis experimental settings.

	Sensitivity Analysis Experiment		
	1	**2**	**3**
Variable	Efficiency -stability coefficient	Average flow	The standard deviation of flow
Scenario(s)	Sensitivity analysis between efficiency -stability coefficient and delay	Sensitivity Analysis between mean traffic flow and delay	Sensitivity analysis between fluctuation and delay of traffic flow
Model(s)	MSD-$r = 0 \sim 0.5$	MSD-$r = 0.3$	MSD-$r = 0.3$

5.1. Efficiency-Stability Coefficient and Bandwidth

The efficiency-stability coefficient r determines the model's preference for efficiency and stability under the condition of emphasizing model stability ($0 \leq r \leq 0.5$). As shown in Figure 14, the influence of the efficiency stability coefficient on the mean and standard deviation of the model delay is discussed. With an increase in r, the standard deviation of delay increases while the average delay decreases. Overall, the inflection point of the delay standard deviation curve appears at $r = 0.3$. When $\gamma > 0.3$, the rising rate of delay standard deviation is fast, which means that the stability of the model is gradually deteriorating, and the decreasing speed of efficiency is relatively stable. To maximize stability without losing overall efficiency, the r in the previous experimental scenario is taken as 0.3.

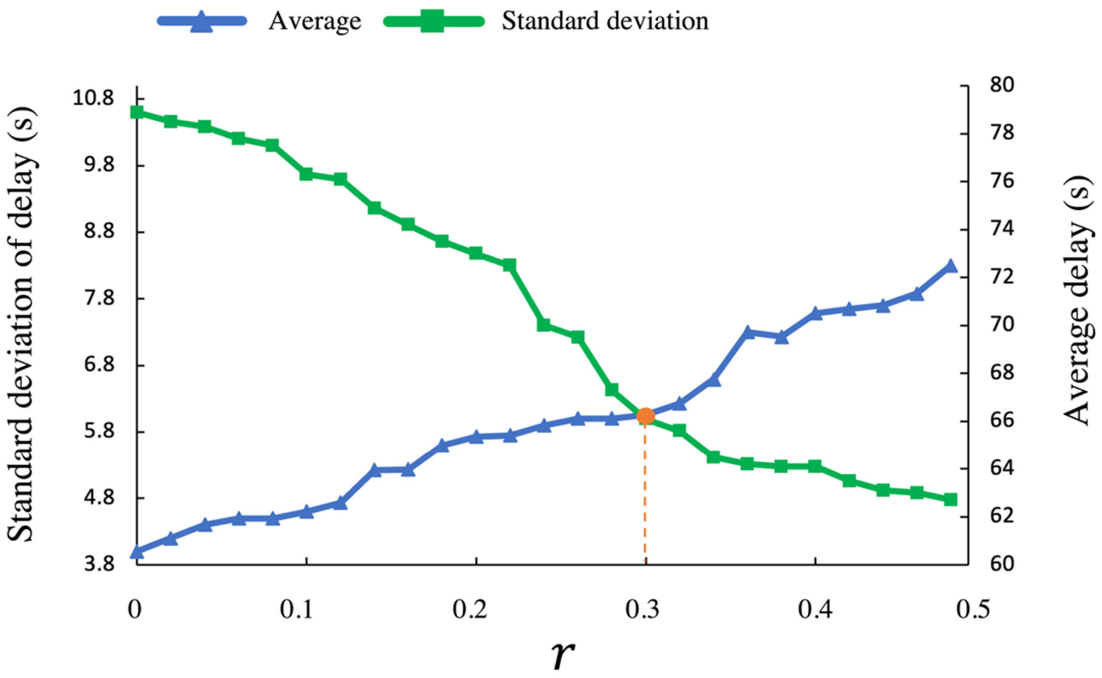

Figure 14. Effect of efficiency stability coefficient on delay.

5.2. Average Traffic Flow and Delay

To explore the influence of a change in the flow mean value on the delay of each model, and to control other parameters to remain constant, according to Table 2, multiply the flow mean value of each direction by the scaling factor, and the scaling range is 0.5~1.5. The results are shown in Figure 15. Overall, an increase in traffic volume causes the overall operation efficiency and stability of each control scheme to be worse, and the slope of the mean and maximum delay increases significantly. With an increase in traffic volume, the distance between the traditional MAXBAND model and the MSD-$r = 0.3$ model in the standard deviation of delay and the maximum delay value gradually increases. It shows that when the flow is large, the stability of the operation efficiency of the traditional control scheme gradually becomes worse, and it is difficult to resist the change in the flow. However, the MSD-$r = 0.3$ model has the slowest growth rate. It can be concluded that the model is less sensitive to changes in external disturbances than the other models, which shows that the model has good stability.

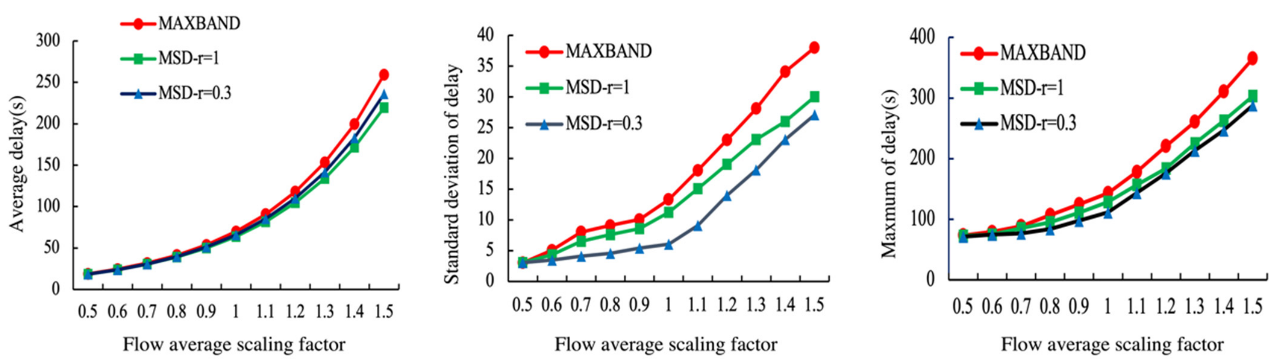

Figure 15. Effect of traffic flow on delay index.

5.3. Fluctuation of Traffic Flow and Delay

Similarly, to study the impact of a change in flow standard deviation on the delay of each model and to control other parameters to remain constant, according to Table 2, multiply the flow standard deviation of each flow direction by the scaling factor, which ranges from 0.5 to 1.5. The results are shown in Figure 16. It is found that an increase in the fluctuation degree of traffic demand causes the overall operation efficiency and stability of each control scheme to be gradually worse, and the standard deviation and maximum value of delay change significantly. For the average delay, MAXBAND has a good effect when the fluctuation of traffic demand is slight. However, with an increase in traffic flow fluctuation, the average traffic flow cannot represent the overall traffic operation scenario well, and the average delay controlled by MAXBAND increases significantly.

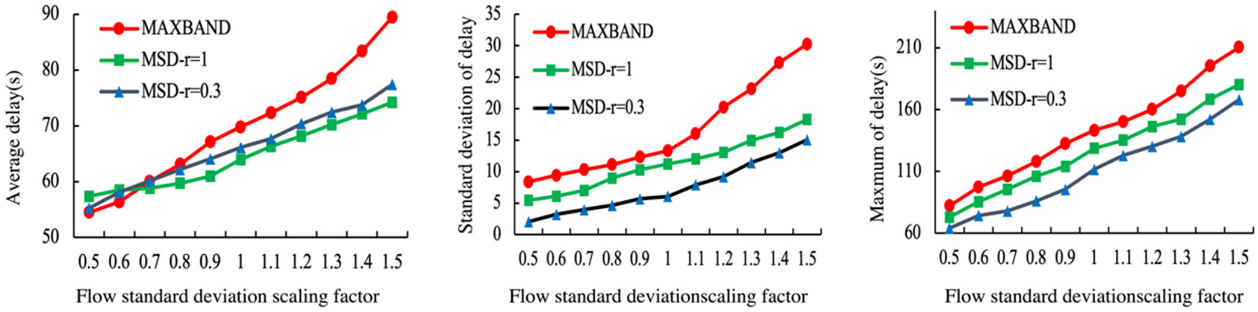

Figure 16. Effect of traffic flow fluctuation on delay index.

6. Conclusions

The existing multi-path arterial signal model is more sensitive to traffic input changes such as flow and signal timing. Its adaptability to fluctuations of traffic input in actual traffic scenarios needs to be improved. In this study, a heuristic approach for a multi-path model considering fluctuations of traffic flow is proposed, which takes the phase sequence and offset of each intersection as the decision variables and takes the weighted optimization of the efficiency and stability of the model as the objective. By adjusting the efficiency stability coefficient to control the model's preference for efficiency and stability, the following conclusions can be drawn in combination with the test results:

(1) The mean, standard deviation (MSD-$r = 0.3$) model performs well in the standard deviation and maximum value of each index on the premise of less deterioration of delay, parking times, average speed, and other indicators, thus, significantly improving the stability of the overall operation effect. Among them, the deterioration degree of the average value of each index is only 3.32%. The results of the comparison analysis shows that the standard deviation of the overall index is improved by 45.4%, and the maximum value is improved by 13.2%.

(2) As compared with the traditional MAXBAND model and the MSD-r = 1 model, the average standard deviation (MSD-$r = 0.3$) model performs better in the stability of the mean, standard deviation, maximum, and other indicators of delay when the mean and standard deviation of traffic flow fluctuates, and the overall stability of the model is superior.

The heuristic method under traffic uncertainty proposed in this paper is essentially a multi-scenario deterministic model. In future research, robust optimization theory can be combined with it to consider the performance of the model under worst traffic scenarios.

Author Contributions: Conceptualization, G.R.; Methodology, T.H. and W.C.; Software, W.C.; Validation, C.D.; Formal analysis, T.H. and W.C.; Resources, G.R.; Data curation, W.C. and Q.C.; Writing—original draft, T.H.; Writing—review & editing, T.H.; Visualization, C.D.; Project administration, Q.C. All authors have read and agreed to the published version of the manuscript.

Funding: This work was partly supported by the National Key Research and Development Program of China under Grant 2019YFB1600200, the National Key Research and Development Program of China under Grant 2016YFE0206800, and the National Nature Science Foundation of China under Grant 52072068.

Data Availability Statement: Not applicable.

Acknowledgments: We want to thank all the team members of Renyi Men for their insightful comments, which significantly improved the quality of the analysis and presentation of this study.

Conflicts of Interest: The authors declare no conflict of interest.

References

1. Morgan, J.T.; Little, J.D.C. Synchronizing Traffic Signals for Maximal Bandwidth. *Oper. Res.* **1964**, *12*, 896–912. [CrossRef]
2. Little, J. The Synchronization of Traffic Signals by Mixed-Integer Linear Programming. *Oper. Res.* **1966**, *14*, 568–594. [CrossRef]
3. Little, J.; Kelson, M.; Gartner, N. MAXBAND: A Program for Setting Signals on Arteries and Triangular Networks. *Transp. Res. Rec. J. Transp. Res. Board* **1981**, *795*, 40–46.
4. Chang, E.; Cohen, S.; Liu, C.; Chaudhary, N.A.; Messer, C. MAXBAND-86. Program for optimizing left-turn phase sequence in multicriterial closed networks. *Transp. Res. Rec.* **1988**, *1181*, 61–67.
5. Pillai, R.S.; Rathi, A.K. *MAXBAND Version 3.1: Heuristic and Optimal Approach for Setting the Left Turn Phase Sequences in Signalized Networks*; University of North Texas Libraries: Denton, TX, USA, 1995.
6. Gartner, N.H.; Assman, S.F.; Lasaga, F.; Hou, D.L. A multi-band approach to arterial traffic signal optimization. *Transp. Res. Part B Methodol.* **1991**, *25*, 55–74. [CrossRef]
7. Stamatiadis, C.; Gartner, N. MULTIBAND-96: A program for variable bandwidth progression optimization of multicriterial traffic networks. *Transp. Res. Rec.* **1996**, *1554*, 9–17. [CrossRef]
8. Cesme, B.; Furth, P.G. Self-organizing traffic signals using secondary extension and dynamic coordination. *Transp. Res. Part C Emerg. Technol.* **2014**, *48*, 1–15. [CrossRef]
9. Gomes, G. Bandwidth Maximization Using Vehicle Arrival Functions. *IEEE T Intell Transp.* **2015**, *16*, 1977–1988. [CrossRef]
10. Zhang, C.; Xie, Y.; Gartner, N.H.; Stamatiadis, C.; Arsava, T. AM-Band: An Asymmetrical Multi-Band model for arterial traffic signal coordination. *Transp. Res. Part C Emerg. Technol.* **2015**, *58*, 515–531. [CrossRef]
11. Yang, X.; Cheng, Y.; Chang, G.-L. A multi-path progression model for synchronization of arterial traffic signals. *Transp. Res. Part C Emerg. Technol.* **2015**, *53*, 93–111. [CrossRef]
12. Chen, Y.; Cheng, Y.; Chang, G. Design of an arterial signal progression plan for multi-path flows with only intersection turning counts. *Transp. Res. Part C* **2021**, *130*, 103322. [CrossRef]
13. Li, C.; Wang, H.; Lu, Y. A multi-path arterial progression model with variable signal structures. *Transp. A Transp. Sci.* **2022**, 1–35. [CrossRef]
14. Arsava, T.; Xie, Y.; Gartner, N. OD-NETBAND: An Approach for Origin–Destination Based Network Progression Band Optimization. *Transp. Res. Rec. J. Transp. Res. Board* **2018**, *36*, 863080060. [CrossRef]
15. Lin, Y.; Yang, X.; Zou, N. Passive transit signal priority for high transit demand: Model formulation and strategy selection. *Transp. Lett.* **2019**, *11*, 119–129. [CrossRef]
16. Wei, W.; Chen, F. Optimal Control for IsolatedIntersection Signal Based on Genetic Algorithm. *Comput. Eng.* **2007**, *33*, 217–219.
17. Sheffi, Y.; Powell, W.B. Optimal Signal Settings Over Transportation Networks. *J. Transp. Eng.* **1983**, *109*, 824–839. [CrossRef]
18. Heydecker, B. Uncertainty and variability in traffic signal calculations. *Transp. Res. Part B* **1987**, *21*, 79–85. [CrossRef]
19. Wang, Q.; Tan, X.; Zhang, S. SignalTiming Optimization of Urban Single-point Intersections. *J. Traffic Transp. Eng.* **2006**, *6*, 60–64.
20. Li, J.-Q. Discretization modeling, integer programming formulations and dynamic programming algorithms for robust traffic signal timing. *Transp. Res. Part C* **2010**, *19*, 708–719. [CrossRef]
21. Wada, K.; Usui, K.; Takigawa, T.; Kuwahara, M. An optimization modeling of coordinated traffic signal control based on the variational theory and its stochastic extension. *Transp. Res. Part B* **2017**, *117*, 907–925.
22. Shapiro, A.; Dentcheva, D.; Ruszczynski, A. *Lectures on Stochastic Programming: Modeling and Theory*; Mathematical Programming Society: Philadelphia, PA, USA, 2009.
23. Bazaraa, M.S.; Sherali, H.D.; Shetty, C.M. *Nonlinear Programming: Theory and Algorithms*, 2nd ed.; John Wiley & Sons: New York, NY, USA, 1993.
24. Mulvey, J.M.; Vanderbei, R.J.; Zenios, S.A. Robust Optimization of Large-scale Systems. *Oper. Res.* **1995**, *43*, 264–281. [CrossRef]
25. Lopez, P.A.; Behrisch, M.; Bieker-Walz, L.; Erdmann, J.; Flötteröd, Y.; Hilbrich, R.; Lücken, L.; Rummel, J.; Wagner, P.; Wiessner, E. Microscopic traffic simulation using sumo. In Proceedings of the 2018 21st International Conference on Intelligent Transportation Systems (ITSC), Maui, HI, USA, 4–7 November 2018.